Desalination and Water Treatment
www.deswater.com

doi: 10.5004/dwt.2019.23440

141 (2019) 238–247
February

Creation of novel nanospheres/nanowires from *Beauveria bassiana* and their application for adsorption of Cd(II) in aqueous solution

Haizhou Xu[a,b], Tianli Yang[b], Ren He[b], Wenlei Wang[a,b,*], Gui Zhang[a,b]

[a]*Key Laboratory for Digital Dongting Lake Basin of Hunan Province, Central South University of Forestry and Technology, Changsha 410004, China*
[b]*College of Science, Central South University of Forestry and Technology, Changsha 410004, China,*
email: wenlei_wang@hotmail.com (W. Wang)

Received 24 April 2018; Accepted 6 November 2018

ABSTRACT

In this paper, a novel bio-functional nanomaterial was synthesized based on *beauveria bassiana*. SEM characterization showed that there were two classic morphologies, including nanospheres formed by the spore of *beauveria bassiana* and nanowires originated from the hyphae of *beauveria bassiana*. The experiments were carried out including effect of pH, contact time and Cd(II) initial concentration. Substantial ascent for Cd(II) adsorption capacity by *beauveria bassiana* was observed from pH 3 to 5. With the increase of pH, there was no significant change in the cadmium adsorption. The pseudo-second-order model better presented the adsorption kinetic process. It could be concluded that the dominant mechanism was the chemical adsorption. The Freundlich model could better fit the adsorption isotherms than Langmuir model. The TEM, FT-IR, XRD and XPS analyses were carried out to investigate the adsorption mechanism. TEM characterization showed that Cd(II) element was detected on the surface of nanosphere within amorphous morphology. FT-IR spectra analysis showed that some individual functional groups of the novel bio-functional nanomaterials have changed obviously before and after adsorption. XRD patterns showed that peaks of $2\theta = 13°$, $2\theta = 46°$ and $2\theta = 75.5°$ have disappeared. The reason might be that organic groups of the sample changed due to the adsorption of Cd(II) ions. Based on these results, the adsorption mechanisms could be explained as the formation of $Cd(OH)_2$ and $CdCO_3$ precipitation on the surface of the adsorbent by XPS spectra analysis. The results provided an excellent potential application for the waste fungi produced by the fermentation industry, and provided an important material for the removal of heavy metal ions from wastewater.

Keywords: Beauveria bassiana; Nanospheres/nanowires; Cd(II) adsorption; Adsorption mechanism

1. Introduction

Water contaminated by toxic heavy metal ions such as Cd(II) have becoming a major environmental problem because of its potential accumulation, non-biodegradability. High toxicity in water and soil ecosystems results in a hazardous effect on all living organisms [1,2]. Moreover, the accumulation of cadmium in human bodies can cause itai-itai disease and chronic disorders of the liver, kidney, nervous, and cardiovascular systems [3]. Rapid industrialization was considered as the release of wastewater. Although the usage of cadmium in the industry have been strictly limited, and the demand for cadmium have been reduced year by year, cadmium compounds were still applied in various fields such as pigments [4], batteries [5], solar photocatalysis [6], and elec-trowinning. In some areas, toxic heavy metal ions have still been discharged into the water and soil ecosystems without any treatment [7–10]. As a result, the removal of Cd(II) ions from water and soil have become a very important issue for environmental protection and human health [11,12].

*Corresponding author.

The existing technologies for the elimination of heavy metals from wastewater included chemical precipitation, phyto-extraction, ion exchange, membrane filtration and adsorption [13–18]. Most of these methods took multiple consecutive steps. Therefore, the average removal efficiency was expensive [19]. Among them, adsorption was commonly considered as one of the most proficient techniques due to its apparatus simplicity, high efficiency process, and low costs [20,21]. As early as the 1970s, there were researches about biological adsorbents for wastewater treatment [22]. Gadd and Griffiths [23] carried out the research to examine the nature of the interactions between microbes and heavy metals, and attempted to clarify the environmental and microbial processes underlying resistance or tolerance. The wasting fungi produced by the fermentation industry were potential adsorbents for the adsorption of heavy metal contaminants [24]. Yang et al. [25] developed a reclaimable adsorbent of fungus hyphae-supported alumina (FHSA) bio-nanocomposites, finding that the FHSA had potential applicability in fluoride removal. Natarajan et al. [26] carried out a research that a waste fungal biomass consisted of *aspergillus niger* grown on wheat bran in a solid-state fermentation process, and this waste have been efficiently used in the removal of toxic metal ions such as iron, calcium, nickel and chromium from aqueous solutions. It meant that a large number of low-cost fungi can be obtained from fermentation industry. In many cases, these abundant fungi cells were unwanted byproducts, and these fungi cells were hoped to be turned into treasure. There were a large amount of functional groups in the fungal cell wall contributing to fungal strong adsorption function such as sulfonate, amino, carboxyl, hydroxyl and sulfate groups [27]. Azin and Moghimi [28] indicated that dye removal was performed through biosorption process. Hydroxyl and amine groups in the cell wall polymers had the main role in dye biosorption. Park et al. [29] found that the inactivation of *aspergillus niger* can reduce more toxic Cr^{6+} to almost non-toxic Cr^{3+}. If the time was long enough, Cr^{6+} was no longer present in the aqueous solution, even all the Cr^{6+} adsorbed on the mycelium surface would be transformed to Cr^{3+}. Dwivedi et al. [30] discussed two fungi *aspergillus flavus* and *aspergillus niger* as biosorbent for removal of heavy metals from wastewater and industrial effluents containing higher concentration of heavy metals. Siddiquee et al. [31] discussed about the tolerance and biosorption capacity of filamentous fungi (*Trichoderma harzianum*, *T.aureoviride* and *T.virens*) on Zn^{2+}, Pb^{2+}, Ni^{3+} and Cu^{2+}. Their results indicated the possibilities for the clean-up of heavy metals by using bio-functional materials. Therefore, bio-functional materials obtained based on fungi, bacteria, and so on, did have a certain heavy metal adsorption capacity.

Beauveria bassiana belongs to the Eumycota, Deuteromycotina, Hyphomycetales, Moniliales, Moniliaceae, Beauveria. At present, the research on *beauveria bassiana* mainly focused on the field of biological characteristics and agricultural biocontrol. *Beauveria bassiana* was an important broad-spectrum insect entomopathogenic fungi. Berestetskiy et al. [32] found that the extracts of the *Beauveria bassiana* and *B. pseudobassiana* exhibited a broad spectrum of biological activity. It was also one of the widely studied and applied entomogenous fungi around the world, accounting for about 21% of the total number of entomogenous fungi [33]. In this study, the bio-functional materials based on *beauveria bassiana* were successfully synthesized by a facile and simple method. And then, the novel bio-functional material was analyzed by Fourier transform infrared (FT-IR) spectra, X-ray diffraction (XRD) measurements, X-ray photoelectron spectroscopy (XPS) analyses, scanning electron microscope (SEM), and Transmission electron microscopy (TEM) images. Furthermore, the adsorption capacity of such novel bio-functional material was evaluated by using Cd(II) as a model of heavy metals. The experimental results provided an important reference for *beauveria bassiana* as a bio-functional material for the removal of heavy metal ions from the wastewater, and also provided an outstanding potential application for the wasting fungi produced by the fermentation industry.

2. Experimental section

2.1. Synthesis of fungus Beauveria bassiana

A pure strain of *beauveria bassiana* was obtained from Central South University of Forestry and Technology, Changsha, China. The fungal isolate was maintained on slants of Potato-dextrose-agar (PDA). And freshly revived cultures were used for the synthesis of bio-functional materials. The PDA medium was sterilized at 121°C for 30 min using a high-temperature moist heat sterilization method. After the ultra-violet (UV) sterilizing above the operating room and console for 20 min, a flat plate with 12 cm of diameter was poured with the PDA. After the flat plate cooled, the *beauveria bassiana* was inoculated and cultured for seven days. A small amount of *beauveria bassiana* spores were picked by a vaccination needle to observe under 40 times microscope. *Beauveria bassiana* were successfully cultured if a large number of spores were observed under 40 times microscope. After preparation of *beauveria bassiana* were sufficient, the *beauveria bassiana* obtained above was worked into spore powder under minus 80°C using a freeze-drying method. After BET test, the specific surface area of *beauveria bassiana* was 37.24 cm^3/g. And then, the samples prepared above were used to carry out the next adsorption kinetic and isotherms.

2.2. Chemicals

Cd(II) chloride ($Ca(Cl)_2 \times 2.5H_2O$), sodium hydroxide (NaOH), hydrochloric acid (HCl) were purchased from China national pharmaceutical group corporation. The deionized (DI) water was used in all experiment.

2.3. Instruments

The Cd(II) ion detection was carried out on an Atomic absorption spectrometer (Thermo solaarmb, USA) with an air-acetylene burner. The operating parameters for Cd(II) were set as recommended by the manufacturer. A pH meter, the Amtast AMT12 (USA) model glass-electrode, was employed for measuring pH values in the aqueous phase. Scanning electron microscope (SEM) (Ultra 55, Germany) was used to analyze the size and morphology of the sample in this work. To understand the adsorption mechanism of

Cd(II) on bio-functional material based on *beauveria bassiana*, Fourier transform-infrared spectrometry (FT-IR) spectrophotometer in range of 400–4000 cm^{-1} with the KBr disk method (Thermo Nicolet 5700, USA) was applied to identify the surface functional groups. The structures of samples were analyzed by an X-ray powder diffractometer (XRD) (Bruker D8 Advance, Germany) with Cu Kα radiation at 40 kV and 40 mA in a scanning range of 10°–90° (2θ). XPS analyses were performed with an Axis ultra spectrometer (Kratos Analytical Ltd.) using aluminum (Al) monochromatic X-ray source (AI Ka = 1486.6 eV) at 25°C in a high vacuum environment (approximately 5 × 10^{-9} tor). All the binding energies were calibrated by using containment carb on the C1s (284.8 eV). TEM images were obtained on a Tecnai G2 F20 S-TWIN with an accelerating voltage of 100 kV.

2.4. Adsorption experiment

In the experiments, the 15 mg/L, 30 mg/L, 40 mg/L, 50 mg/L, 60 mg/L, 70 mg/L and 90 mg/L of Cd(II) stock solution were prepared by dissolving an amount of Cd $(Cl)_2 \times 2.5H_2O$ into DI water, respectively. The pH optimization experiments were performed in a 30 mL of 50 mg/L Cd(II) solution contained in a 250 mL conical flask with 0.2000 g of bio-functional material based on *beauveria bassiana*. The conical flask was placed on an orbital shaker at 180 rpm for 360 min (Hanuo instrument SHA-B, China). These experiments have been performed from pH 3 to 8. The adsorption kinetic experiment was performed with 0.2000 g of the sample poured in a conical flask including 30 mL of Cd(II) (50 mg/L) with pH 5. The conical flask was placed on an orbital shaker (Hanuo instrument SHA-B, China) at 180 rpm for 15 min, 60 min, 120 min, 300 min and 720 min, respectively. The adsorption thermodynamics experiments were performed in a 250 mL conical flask with 0.2000 g of the adsorbent and 30 mL of Cd(II) solution with 15 mg/L, 30 mg/L, 40 mg/L, 50 mg/L, 60 mg/L, 70 mg/L and 90 mg/L at pH 5, respectively. The reagent bottle was placed on an orbital shaker (Hanuo instrument SHA-B, China) at 180 rpm for 720 min. The suitable pH of the Cd(II) solution was attained with 0.2 mol/L of HCl or 0.2 mol/L of NaOH. A 0.45 μm syring filter water membrane was applied to filter the suspension. To assess Cd(II) concentration, the filter solution was carried out on an Atomic absorption spectrometer(AAS). The adsorption capacity for Cd(II) uptake, Q_e (mg/g), at equilibrium can be determined by the following Eq. (1) [34]:

$$Q_e = (C_i - C_e)V / M \tag{1}$$

where C_i and C_e (mg/L) refer to Cd(II) concentration at initial and equilibrium, respectively; V (L) was the Cd(II) solution volume, and M (g) was the adsorbent mass.

In this kinetic study, Cd(II) adsorption amount (Q_t) can be calculated by Eq. (2) [35,36]:

$$Q_t = (C_i - C_t)V / M \tag{2}$$

where C_i and C_t (mg/L) were Cd(II) concentration at initial and time t (min), respectively; V (L) was the Cd(II) solution volume, and M (g) was the adsorbent mass.

2.5. Adsorption model fitting

In this work, the pseudo-first-order and pseudo-second-order kinetic models were applied to describe the adsorption of Cd(II) ions onto bio-functional materials based on *beauveria bassiana*. The pseudo-first-order kinetic model was given as Eq. (3) [37,38]:

$$\ln(Q_e - Q_t) = \ln Q_e - K_1 t \tag{3}$$

The pseudo-second-order kinetic model defined the adsorption mechanism. It can be articulated by the subsequent Eq. (4) [39,40]:

$$t/Q_t = 1/K_2 Q_e^2 + t/Q_e \tag{4}$$

where Q_t and Q_e (mg/g) were the amounts of the metal adsorbed at time t (min) and equilibrium, respectively. K_1 (1/min) was the rate constant of pseudo-first-order, and K_2 (g/(mg×min)) was the rate constant of pseudo-second-order models.

The intra-particle-diffusion model (IPD model) was proposed to determine whether Intra-particle diffusion was the rate limiting step. It can be articulated by the subsequent Eq. (5) [41]:

$$Q_t = K_{id} t^{0.5} + C \tag{5}$$

where K_{id} was the Intra-particle diffusion rate constant (mg/(g×$min^{0.5}$)), C was a constant related to the boundary layer thickness. If the rate limiting step was the Intra-particle diffusion, the plot of Q_t against the square root of time should be a straight line and should pass through the origin ($C = 0$). Otherwise, the deviation of the plot from the linearity indicated the rate-limiting step should be boundary layer (film) diffusion.

Most adsorption data can be suitably expressed using either Langmuir or Freundlich model, and the linearized form of these models can be demonstrated in Eq. (6) [42,43] and Eq. (7) [44,45]:

$$C_e/Q_e = 1/K_L Q_{\max} + C_e/Q_{\max} \tag{6}$$

$$\ln Q_e = \ln K_f + 1/n \ln C_e \tag{7}$$

where Q_e was the solid phase equilibrium concentration and C_e was equilibrium concentration of the metal ions (mg/L). Q_{max} was the maximum sorption capacity (mg/g), and K_L was a constant related to binding energy of the sorption system (L/mg). The K_L and Q_{max} can be obtained from the intercept and slope of the linear plots when C_e/Q_e results in a fairly straight line. Also, K_f and $1/n$ were related to the Freundlich equilibrium constant. K_f (mg/g)(mg/L)$^{1/n}$ was the Freundlich constant linked with the relative capacity, and n corresponded to adsorption intensity.

3. Results and discussion

3.1. Characterization of bio-functional materials

3.1.1. SEM characterization

Fig. 1 shows the SEM images of bio-functional materials. As illustrated in Fig. 1a, there were two classic morphol-

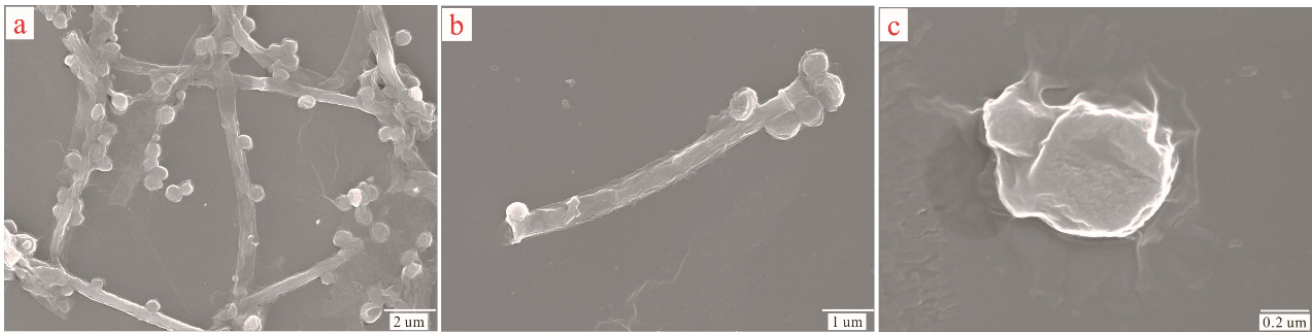

Fig. 1. SEM images of BB Nanomaterials. (a) two classic morphologies of samples; (b) nanospheres arranged around the nanowire; (c) the nanosphere of BB Nanomaterials.

ogies in the visualization of samples. One was in the form of nanosphere formed by the spores of *beauveria bassiana* and another one was in the form of nanowire originated from the hyphae of *beauveria bassiana*. Thus, the bio-functional materials would be named as BB Nanomaterials in this work. The diameter of nanospheres were between 460–760 nm. It can be observed obviously the nanospheres attached around the nanowires, as a result of that the spores of *beauveria bassiana* fall off from the hyphae of *beauveria bassiana*, during the synthesis of the sample. Fig. 1b shows the attachment phenomena that six nanospheres arranged around the nanowire in the form of monolayer and non-uniform. The diameters of nanospheres were approximately 580 nm. While, the width of nanowire was approximately 500 nm and the length was 5.5 um. As presented in Fig. 1c, the nanosphere of BB Nanomaterials emerged in the form of spherical. In general, the adsorption of metal ions from solution was influenced by surface chemistry, sorbent surface and precipitation reactions [46]. The surface of the BB Nanomaterials was rough, which could effectively increase the specific area and increase the adsorption capacity of the sample. The reason for that might be due to the dehydration in the freeze-drying process of *beauveria bassiana*.

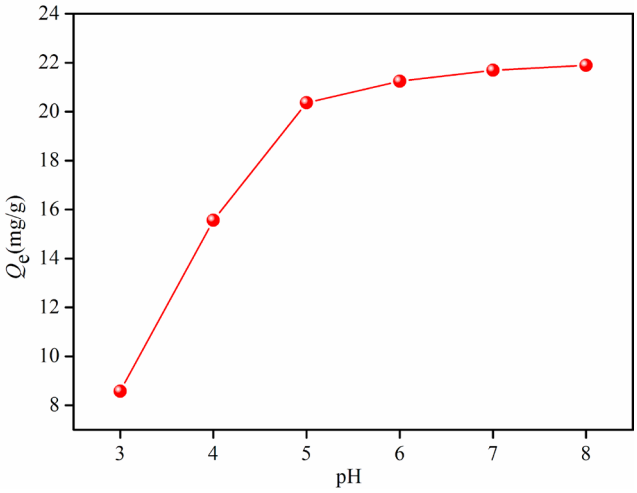

Fig. 2. Effect of aqueous solution pH on adsorption of Cd(II) (at 298.1 K; adsorbent = 0.2000 g; pH = 3, 4, 5, 6, 7 and 8; *C* (Cd) = 50 mg/L; *V* = 30 Ml; agitation speed = 180 rpm; contact time = 360 min).

3.2. Removal of Cd(II) by bio-functional materials

3.2.1. Effect of pH

pH played a significant role in heavy metal removal by fungus [47], which could affect the speciation of the metal in the solution as well as the surface properties of the fungus. Generally, pH could affect adsorption capacity by affecting ion exchange and metal deposition reactions, or by influencing the electric charge density of the surface to facilitate, or hinder electrostatic interactions to influence metal ion concentrations in aqueous solution [48]. To determine the effect of the initial solution pH on Cd(II) adsorption with the BB Nanomaterials as adsorbent, the pH from 3 to 8 of the aqueous solution were systematically carried out in the 50 mg/L of Cd(II) aqueous solution for the contact time of 360 min. The desired pH was adjusted by adding droplets 0.2 mol/L of HCl or NaOH. As shown in Fig. 2, substantial ascent in Cd(II) adsorption capacity by *beauveria bassiana* was observed from pH 3 to 5. Cd(II) removal had no significant alternation from pH 5 to 8. Lower adsorption capacity at low pH might be ascribed to the association of hydronium ions with the cell surface [49]. The hydronium ions with the cell surface generated a positive charge on the fungus cell wall. Thus, BB Nanomaterials with positive charge on the cell wall created a repulsive force against Cd(II) ions in the solution. In general, Q_e reached the maximum adsorption capacity after pH 5. Thus, pH 5 was selected as the optimum pH in this paper.

3.2.2. Adsorption kinetic and breakthrough test

Adsorption kinetics were necessary to investigate the adsorption efficiency of sorbents in the removal of Cd(II). Adsorption kinetic experiments are shown in Fig. 3. The adsorption capacity of Cd(II) raised up sharply in the first 120 min and slowly reached saturation at approximately 300 min. Three models including pseudo-first-order, pseudo-second-order and Intra-particle-diffusion equations were used to study the variations in adsorption with time. Through these methods, a proper mechanism to describe the adsorption of Cd(II) ions onto BB nanomaterials was observed. The data were obtained by fitting these models and tabulated in the Table 1. Based on the results, the

pseudo-second-order model presented better correlation coefficient values (R^2 = 0.9948) than those of the pseudo-first-order and Intra-particle-diffusion models because of a higher correlation. Furthermore, the experimental Q_t values possessed good similarity with the theoretical ones. The pseudo-second-order model also better described the kinetics of Cu, Cd and Pb adsorption by the peat moss-derived biochar [50,51], which assumed that the adsorption capacity was proportional to the number of chemical actively sites occupied on the sorbent [39]. Thus, it could be concluded that the dominant mechanism was the chemical adsorption that can be well attributed to the pseudo-second-order kinetic model. In order to further supplement the kinetic experiments and verify the adsorption experiments. After ultrasonic breakthrough, the samples were used for adsorption experiments. As shown in Fig. 4, the adsorption capacity was 21.55 mg/g at 720 min, which was basically similar to the synthesized sample.

3.2.3. Adsorption thermodynamics

As was known to all, the fitting of adsorption isotherm equation to experimental data was often an important aspect of data analysis [52,53]. The most important information that disclosed the adsorbate molecules distribution between the solid and the liquid phases could be provided by the adsorption isotherm when the adsorption process approached equilibrium. A large number of studies have reported problems in linearization of isotherm equations which may lead to violation of the theories behind the isotherm [54–56]. To estimate the adsorption thermodynamics, a different initial concentration of Cd(II) was prepared at pH 5. Also, the most appropriate time was 720 min at 298.1 K. The adsorption isotherms are shown in Fig. 5. The adsorption capacity raised up drastically at first and then stayed unchanged. In this paper, the Langmuir and Freundlich thermodynamics models were used to describe the adsorption actions and adsorption ability of Cd(II) ions onto the BB Nanomaterials.

3.3. Adsorption mechanism

3.3.1. TEM characterization

With the aim of collecting more information about the microstructure and morphology of the BB Nanomaterials, TEM have been employed for analyzing the elemental distribution and lattice distribution with the results shown in Fig. 6. EDX was used to analyze the elemental distribution in order to identify how Cd(II) ions was adsorbed onto BB Nanomaterials. Fig. 6a shows the structure of nanosphere very clearly and retained spore integrity. And, the surface of the spores was thick cell wall with rough wrinkles. Also, the diameter of the nanosphere was approximately 750 nm. As illustrated in Fig. 6b, Cd(II) element was detected on the surface of nanospheres, further proving that novel BB Nanomaterials that originated from *beauveria bassiana* can be used to remove heavy metal ions. As shown in Fig. 6c, HR-TEM had not obvious lattice, proving that the bio-func-

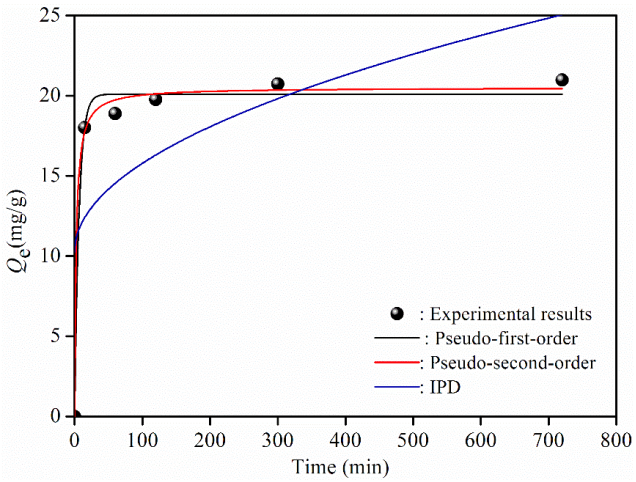

Fig. 3. Adsorption kinetic for adsorption of Cd(II) onto BB Nanomaterials (at 298.1 K; absorbent = 0.2000 g; *C* (Cd) = 50 mg/L; *T* = 15 min, 60 min, 120 min, 300 min and 720 min; *V* = 30 mL; agitation speed = 180 rpm; pH = 5).

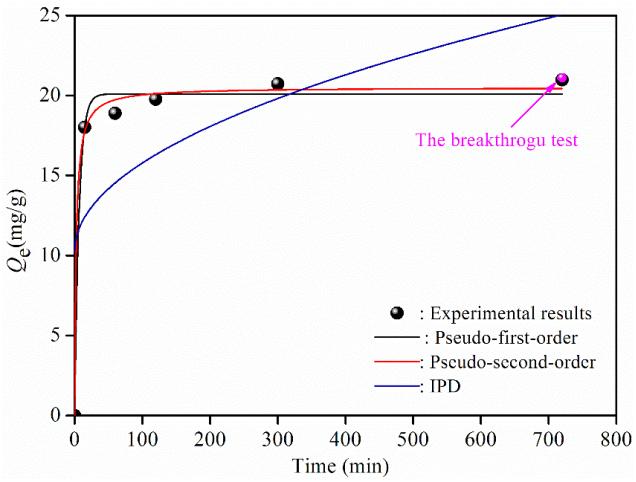

Fig. 4. Adsorption kinetic for adsorption of Cd(II) onto nanoparticles after ultrasonic breakthrough (at 298.1 K; absorbent = 0.2000 g; *C* (Cd) = 50 mg/L; *T* = 15 min, 60 min, 120 min, 300 min and 720 min; *V* = 30 mL; agitation speed = 180 rpm; pH = 5).

Table 1
Kinetic parameters for adsorption of Cd(II) onto BB nanomaterials

Pseudo-first-order			Pseudo-second-order			Intra-particle diffusion		
K_1 (min^{-1})	Q_e (mg/g)	R^2	K_2 (g/mg min)	Q_e (mg/g)	R^2	K_{id}	C	R^2
0.1510	20.0893	0.9895	0.0208	20.5044	0.9948	0.5510	10.2654	0.2960

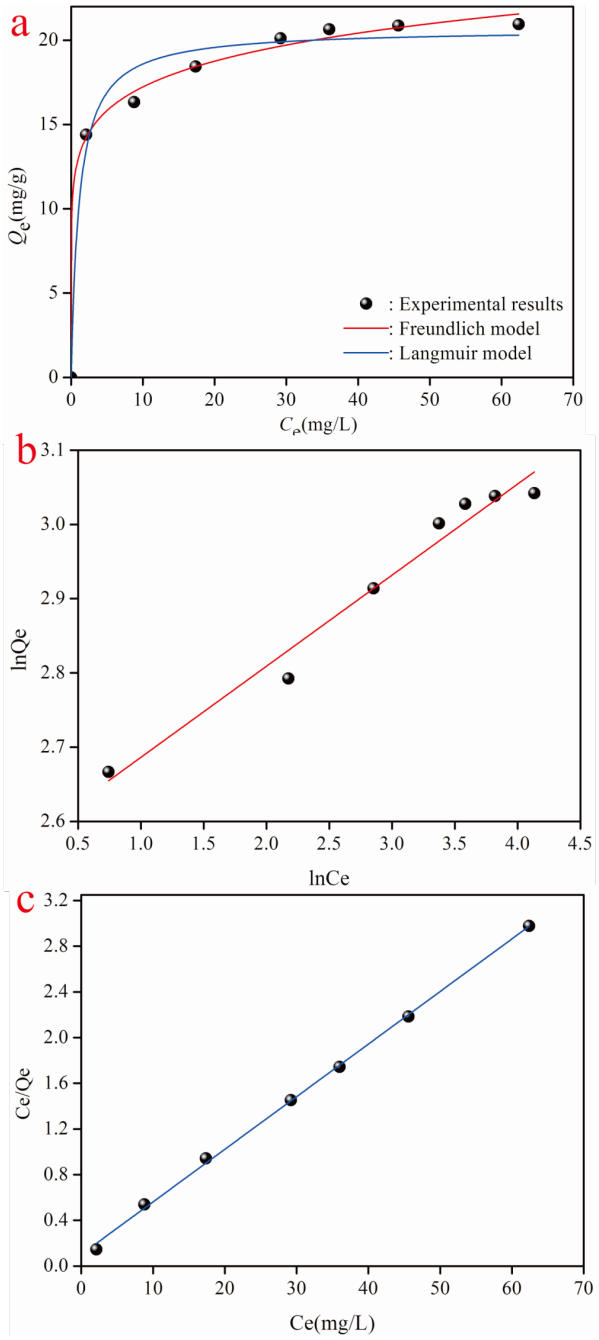

Fig. 5. Adsorption thermodynamics for adsorption of Cd(II) onto BB Nanomaterials (absorbent = 0.2000 g; *C*(Cd) = 15 mg/L, 30 mg/L, 40 mg/L, 50 mg/L, 60 mg/L, 70 mg/L and 90 mg/L; *T* = 720 min; *V* = 30 Ml; agitation speed = 180 rpm; pH = 5). (a) Adsorption thermodynamics for adsorption of Cd(II) onto BB Nanomaterials; (b) Freundlich model for adsorption of Cd(II) onto BB Nanomaterials; (c) Langmuir model for adsorption of Cd(II) onto BB Nanomaterials.

tional materials have not form inorganic salt morphology. That was to say, there was no inorganic salt morphology of the BB Nanomaterials, proving that adsorption of Cd(II) onto the BB Nanomaterials had not significant effect on the composition of the bio-functional materials.

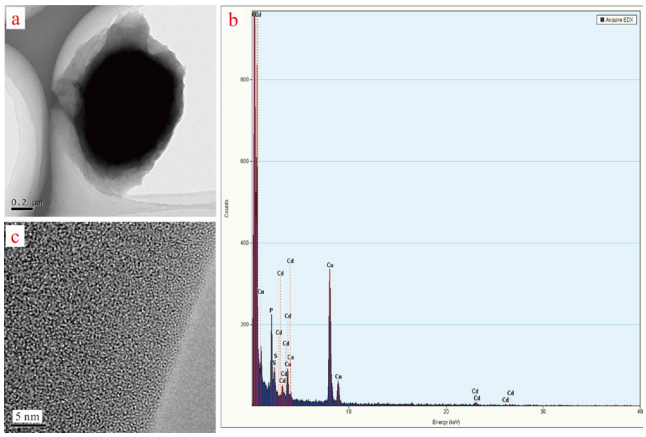

Fig. 6. (a) TEM image of the novel BB Nanomaterials; (b) EDX spectrum of the elemental distribution; (c) HR-TEM image of the novel BB Nanomaterials.

3.3.2. FT-IR and XRD analysis

FT-IR spectra of BB Nanomaterials before and after adsorption were obtained in the range of 500–4000 cm^{-1} (as shown in Fig. 7a). FT-IR gave the possible information on functional group present on the cell surface and their interaction with the heavy metals. Significant, shift in the nature of FT-IR spectra bands of fungi grown with heavy metal were obtained. There are five individual adsorption peaks in Fig. 7a. The characteristic peak of the BB Nanomaterials before and after adsorption in Fig. 7a at 3416 cm^{-1} representing primary and secondary amine and amide for N-H and O-H stretching vibration. The characteristic peak at 2924 cm^{-1} for lipid C-H stretching vibration area, whereas band at 1652 cm^{-1} was protein amide I band and amide II band mainly. The broad band at 1042 cm^{-1} was polysaccharide and other carbohydrate molecules C-O-C and C-O-P stretching vibration band mainly. The broad band at R1 and R2 regions BB Nanomaterials before and after adsorption had individually obvious change. The reason might be that organic groups of BB Nanomaterials changed due to the adsorption of Cd(II) ions onto BB Nanomaterials. The results in this paper were similar to the study of Gola et al. [47] and Kaushik et al. [47]. Moreover, small shifts in every wavelength were observed in presence of metal system, indicating the involvement of various functional groups.

Cd(II) was analyzed by XRD to define its crystal structure. XRD analysis was mainly used for mineral and other compound which had definite crystal structures. XRD patterns for the BB Nanomaterials are presented in Fig. 7b. The different analyses were found that there were individually obvious changes of BB Nanomaterials before and after adsorption. And the changes were mainly reflected in S1, S2 and S3 regions. In the XRD pattern of the BB Nanomaterials after adsorption, peaks of 2θ = 13° in S1 region and 2θ = 75.5° in S3 region have disappeared. Also, a higher peak of 2θ = 46° has also disappeared in the XRD pattern of BB nanomaterials after adsorption, as illustrated in the region S2 in Fig. 7b. The reason might be that the disappearance of organic groups for BB Nanomaterials have been changed due to the adsorption of Cd(II) ions onto the BB nanomaterials.

3.3.3. XPS analysis

The XPS wide scan and different elements core-level spectra of BB nanomaterials after adsorption were employed to further investigate the function group information. The wide scan spectra for BB nanomaterials after adsorption are shown in Fig. 8a, which shows O 1s, Cd 3d, C 1s, Si 2p and Al 2p signal with binding energy centered at 531.6 eV, 405.2 eV, 284.1 eV, 105.3 eV and 84.5 eV, respectively. This implied that Cd(II) ions have successfully conjugated in BB Nanomaterials after adsorption. As illustrated in Fig. 8b, two peak components of the Cd 3d core-level spectra of BB Nanomaterials after adsorption had binding energies at about 404.4 eV and 405 eV, which can be assigned to CdO (48.71 wt. %) and $Cd(OH)_2$ (51.29 wt. %) respectively, proving that BB Nanomaterials after adsorption have successfully adsorbed Cd(II) ions. Moreover, the XPS C 1s core-level spectra of BB nanomaterials after adsorption are shown in Fig. 8c. The binding energy centered at approximately 284.098 eV, 285.623 eV, 287.257 eV and 286.401 eV can be assigned to C-C (45.37 wt. %), C=O (29.37 wt. %), CO_3^{2-} (13.77 wt. %) and C-O (11.49 wt. %) species, respectively. The appearance of CO_3^{2-} indi-

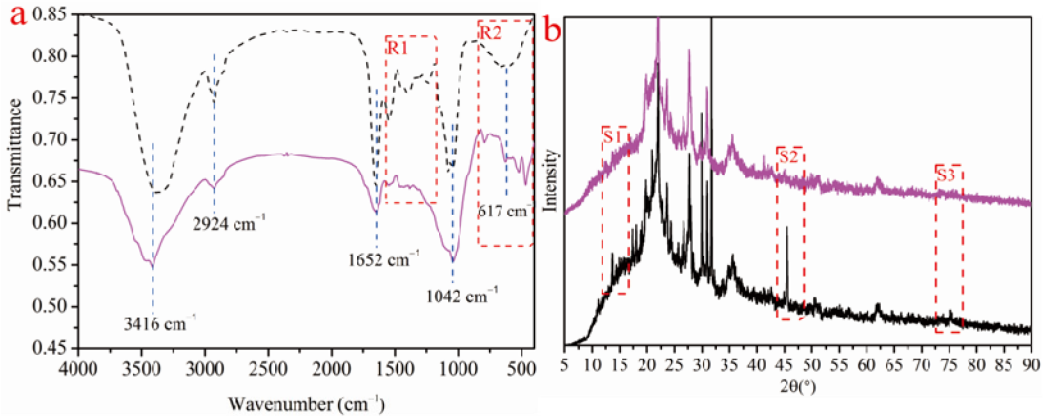

Fig. 7. (a) FT-IR spectra of BB Nanomaterials before and after adsorption (black line represented BB Nanomaterials before adsorption; purple line represented BB Nanomaterials after adsorption). (b) XRD patterns of BB Nanomaterials before and after adsorption (black line represented BB Nanomaterials before adsorption; purple line represented BB Nanomaterials after adsorption).

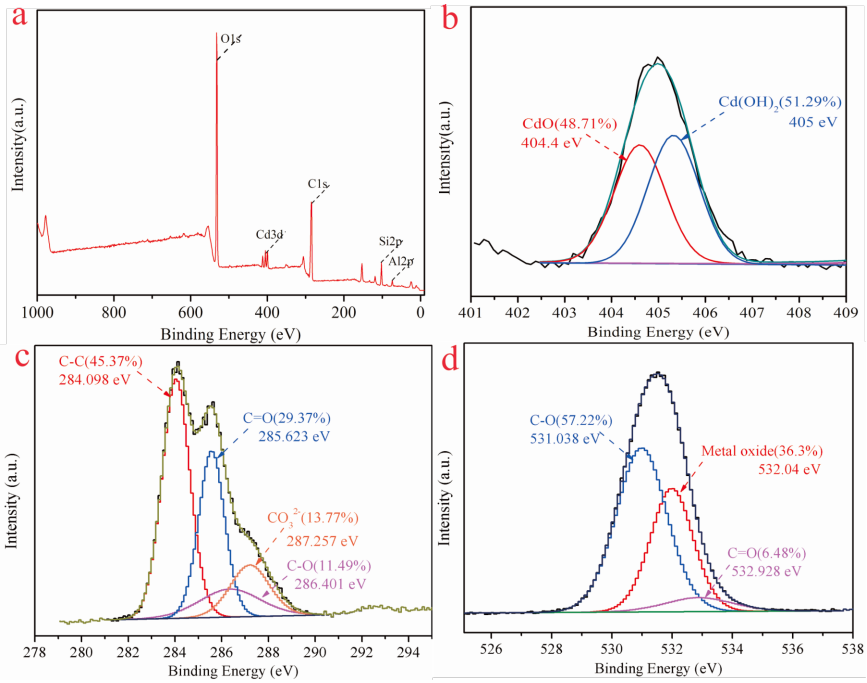

Fig. 8. XPS spectra of BB Nanomaterials after adsorption. (a) XPS spectra of BB Nanomaterials after adsorption of Cd(II); (b) Cd 3d spectra of BB Nanomaterials after adsorption; (c) C 1s spectra of BB Nanomaterials after adsorption; (d) O 1s spectra of BB Nanomaterials after adsorption.BB Nanomaterials.

Table 2
Thermodynamics parameters for adsorption of Cd(II) onto BB Nanomaterials

Freundlich model parameters			Langmuir model parameters		
K_f(mg/g) (mg/L)$^{1/n}$	n	R^2	K_L (L/mg)	Q_{max} (mg/g)	R^2
12.9880	0.1226	0.9957	0.8958	20.6604	0.9761

cated that CdO might exist in the form of $CdCO_3$. And also, there were organic materials in BB nanomaterials. As shown in Fig. 8d, two peak components of the O 1s core-level spectra of BB Nanomaterials after adsorption had binding energies at about 531.038 eV, 532.04 eV and 532.928 eV, which could be assigned to C-O (57.22 wt. %), metal oxide (36.3 wt. %) and C=O (6.48 wt. %) species respectively, further demonstrating BB Nanomaterials after adsorption have successfully adsorbed Cd(II) ions.

4. Conclusions

In this paper, one kind of novel BB nanomaterials of bio-functional material is synthesized on the PDA medium based on *beauveria bassiana*. SEM characterization show that there are two classic morphologies in the visualization of samples, including nanosphere formed by the spore of *beauveria bassiana* and nanowire originate from the hyphae of *beauveria bassiana*. A batch of adsorption experiment is carried out including effect of pH, contact time and initial Cd(II) ions concentration. pH 5 is selected as the optimum pH due to the fact that Q_e reached the maximum adsorption capacity after pH 5. In adsorption kinetic, the pseudo-second-order model better presented correlation coefficient values (R^2 = 0.9948). It could be concluded that the dominant mechanism is the chemical adsorption. In adsorption thermodynamics, the Freundlich model could better fit the adsorption isotherms than Langmuir model. In order to explain their adsorption mechanism, analyses of TEM, FT-IR, XRD and XPS are carried out. TEM characterization show that Cd(II) element is detected on the surface of nanosphere within amorphous morphology. FT-IR spectra analyses show that BB nanomaterials before and after adsorption have individually obvious changes. XRD pattern show that peaks of 2θ = 13° in S1 region, 2θ = 75.5° in S3 region and 2θ = 46° in S2 region have disappeared. The reason might be that organic groups of BB Nanomaterials change due to the adsorption of Cd(II) ions onto BB nanomaterials. XPS spectra analyses imply that Cd(II) ions have successfully conjugated in BB nanomaterials after adsorption in form of $CdCO_3$ and $Cd(OH)_2$. In this paper, the preparation process of BB nanomaterials was complicated. However, the novel nanospheres/nanowires created from *beauveria bassiana* comes from the wasting fungi. It will be a significant economical and environment-friendly approach for the reuse of wasting fungi. This work will provide an important material for the removal of heavy metal ions from the wastewater.

Acknowledgments

The authors gratefully acknowledge the financial support of the National Natural Science Foundation of China (Grant No: 21607176), the Natural Science Foundation of Hunan Province, China (Grant No. 2017JJ3516), the Research Foundation of Education Bureau of Hunan Province, China (Grant No. 16B274), the Open fund for key discipline of Forestry of Central South University of Forestry and Technology (Grant No. 2016ZD11), the Science and Technology Planning Project of Hunan Province, China (No. 2016SK2088), and the Youth Scientific Research Foundation of Central South University of Forestry and Technology (104|0329).

Conflicts of interest

The authors declare no conflict of interest.

References

[1] P. Dey, D. Gola, A. Mishra, A. Malik, D.K. Singh, N. Patel, M.V. Bergen, N. Jehmlich, Comparative performance evaluation of multi-metal resistant fungal strains for simultaneous removal of multiple hazardous metals, J. Hazard. Mater., 318 (2016) 679–685.
[2] L. Hernandez, A. Probst, J.L. Probst, E. Ulrich, Heavy metal distribution in some French forest soils: evidence for atmospheric contamination, Sci. Total Environ., 312 (2003) 195–219.
[3] S. Ke, X.Y. Cheng, J.Y. Zhang, W.J. Jia, H. Li, H.F. Luo, P.H. Ge, Z.M. Liu, H.M. Wang, J.S. He, Z.N. Chen, Estimation of the benchmark dose of urinary cadmium as the reference level for renal dysfunction: a large sample study in five cadmium polluted areas in China, BMC Public Health., 15 (2015) 656–665.
[4] L. Giacopetti, A. Satta, Reactivity of Cd-yellow pigments: Role of surface defects, Microchem. J., 137 (2018) 502–508.
[5] M. Abulikemu, J. Barbe, A.E. Labban, J. Eid, S.D. Gobbo, Planar heterojunction perovskite solar cell based on CdS electron transport layer, Thin Solid Films, (2017) doi: 10.1016/j.tsf.2017.07.003.
[6] M.A. Kamran, A. Majid, T. Alharbi, M.W. Iqbal, K. Ismail, G. Nabi, Z.A. Li, B. Zou, Novel Cd-CdS micro/nano heterostructures: Synthesis and luminescence properties, Opt. Mater., 73 (2017) 527–534.
[7] M. Fawzy, M. Nasr, S. Adel, H. Nagy, S. Helmi, Environmental approach and artificial intelligence for Ni(II) and Cd(II) biosorption from aqueous solution using *Typha domingensis* biomass, Ecol. Eng., 95 (2016) 743–752.
[8] M.E. Mahmoud, N.A. Fekry, M.M.A. El-Latif, Nanocomposites of nanosilica-immobilized-nanopolyaniline and crosslinked nanopolyaniline for removal of heavy metals, Chem. Eng. J., 304 (2016) 679–691.
[9] G. Mohammadnezhad, R. Soltani, S. Abad, M. Dinari, A novel porous nanocomposite of aminated silica MCM-41 and nylon-6: Isotherm, kinetic, and thermodynamic studies on adsorption of Cu(II) and Cd(II), J. Appl. Polym. Sci., 134 (2017) 45383–45394.
[10] J.H. Zhao, J. Liu, N. Li, W. Wang, J. Nan, Z.W. Zhao, F.Y. Cui, Highly efficient removal of bivalent heavy metals from aqueous systems by magnetic porous Fe_3O_4-MnO_2: adsorption behavior and process study, Chem. Eng. J., 304 (2016) 737–746.
[11] M. Farasati, S. Haghighi, S. Boroun, Cd removal from aqueous solution using agricultural wastes, Desal. Water Treat., 57 (2016) 11162–11172.
[12] J.G. Sheng, W.H. Qiu, B.T. Xu, H. Xu, C. Tang, Monitoring of heavy metal levels in the major rivers and in residents' blood in Zhenjiang City, China, and assessment of heavy metal elimination via urine and sweat in humans, Environ. Sci. Pollut. Res., 23 (2016) 11034–11045.

[13] G. Mohammadnezhad, M. Dinari, R. Soltani, Preparation of modified boehmite/PMMA nanocomposites by *in situ* polymerization and the assessment of their capability for Cu^{2+} ions removal, New J. Chem., 40 (2016) 3612–3621.
[14] H.B. Cui, Y.C. Fan, J. Yang, L. Xu, J. Zhou, Z.Q. Zhu, *In situ* phytoextraction of copper and cadmium and its biological impacts in acidic soil, Chemosphere, 161 (2016) 233–241.
[15] C.G. Lee, J.A. Park, J.W. Choi, S.O. Ko, S.H. Lee, Removal and recovery of Cr(VI) from Industrial Plating wastewater using fibrous anion exchanger, Water Air Soil Pollut., 227 (2016) 287–297.
[16] M.M. Li, Y.M. Gong, A.C. Lyu, Y.F. Liu, H. Zhang, The applications of populus fiber in removal of Cr(VI) from aqueous solution, Appl. Surf. Sci., 383 (2016) 133–141.
[17] G.Y. Zeng, Y. He, Y.Q. Zhan, L. Zhang, P. Yang, C.L. Zhang, Z.X. Yu, Novel polyvinylidene fluoride nanofiltration membrane blended with functionalized halloysite nanotubes for dye and heavy metal ions removal, J. Hazard. Mater., 317 (2016) 60–72.
[18] H.H. Du, W.L. Chen, P. Cai, X.M. Rong, X.H. Feng, Q.Y. Huang, Competitive adsorption of Pb and Cd on bacteria-montmorillonite composite, Environ. Pollut., 218 (2016) 168–175.
[19] M. Visa, A.M. Chelaru, Hydrothermally modified fly ash for heavy metals and dyes removal in advanced wastewater treatment, Appl. Surf. Sci., 303 (2014) 14–22.
[20] B. Rezaei, O. Rahmanian, Direct nanolayer preparation of molecularly imprinted polymers immobilized on multiwalled carbon nanotubes as a surface-recognition sites and their characterization, J. Appl. Polym. Sci., 125 (2012) 798–803.
[21] X.M. Ma, J.G. Lee, Y. Deng, A. Kolmakov, Interactions between engineered nanoparticles (ENPs) and plants: Phytotoxicity, uptake and accumulation, Sci. Total Environ., 408 (2010) 3053–3061.
[22] G.M. Gadd, Biosorption: critical review of scientific rationale, environmental importance and significance for pollution treatment, J. Chem. Technol. Biotechnol., 84 (2009) 13–28.
[23] G.M. Gadd, A.J. Griffiths, Microorganisms and heavy metal toxicity, Microb. Ecol., 4 (1977) 303–317.
[24] J.L. Zhou, R.J. Kiff, The uptake of copper from aqueous solution by immobilized fungal biomass, J. Chem. Tech. Biotechnol., 52 (1991) 317–330.
[25] W.C. Yang, S.Q. Tian, Q.Z. Tang, L.Y. Chai, H.Y. Wang, Fungus hyphae-supported alumina: An efficient and reclaimable adsorbent for fluoride removal from water, J. Colloid Interf. Sci., (2017) doi: http://dx.doi.org/10.1016/j.jcis.2017.02.015.
[26] K.A. Natarajan, S. Subramanian, J.M. Modak, Biosorption of heavy metal ions from aqueous and cyanide solutions using fungal biomass, Process Metallurgy, 9 (1999) 351–361.
[27] S.M. Bowman, S.J. Free, The structure and synthesis of the fungal cell wall, BioEssays, 28 (2006) 799–808.
[28] E. Azin, H. Moghimi, Efficient mycosorption of anionic azo dyes by Mucor circinelloides: Surface functional groups and removal mechanism study, J. Environ. Chem. Eng., 6 (2018) 4114–4123.
[29] D. Park, Y.S. Yun, J.H. Jo, J.M. Park, Mechanism of hexavalent chromium removal by dead fungal biomass of Aspergillus niger, Water Res., 39 (2005) 533–540.
[30] S. Dwivedi, A. Mishra, D. Saini, Removal of heavy metals in liquid media through fungi isolated from waste water, Int. J. Sci. Res., 3 (2012) 181–185.
[31] S. Siddiquee, S.N. Aishah, S.A. Azad, S.N. Shafawati, L. Naher, Tolerance and biosorption capacity of Zn^{2+}, Pb^{2+}, Ni^{3+} and Cu^{2+} by filamentous fungi (*Trichoderma harzianum*, *T. aureoviride* and *T. virens*), Adv. Biosci. Biotechnol., 4 (2013) 570–583.
[32] A.O. Berestetskiy, A.N. Ivanova, M.O. Petrova, D.S. Prokof'eva, E.A. Stepanycheva, A.M. Uspanov, G.R. Lednev, Comparative analysis of the biological activity and chromatographic profiles of the extracts of *Beauveria bassiana* and *B. pseudobassiana* cultures grown on different nutrient substrates, Microbiology, 87 (2018) 200–214.
[33] M.G. Feng, T.J. Poprawski, G.G. Khachatourians, Production, formulation and application of the entomopathogenic fungus *beauveria bassiana* for insect control: current status, Biocontrol Sci. Technol., 4 (1994) 3–34.
[34] W.Q. Zhu, W.H. Du, X.Y. Shen, H.J. Zhang, Y. Ding, Comparative adsorption of Pb^{2+} and Cd^{2+} by cow manure and its vermicompost, Environ. Pollut., 227 (2017) 89–97.
[35] H. Chen, J.H. Lin, N. Zhang, L.Z. Chen, S.P. Zhong, Y. Wang, W.G. Zhang, Q.D. Ling, Preparation of MgAl-EDTA-LDH based electrospun nanofiber membrane and its adsorption properties of copper(II) from wastewater, J. Hazard. Mater., 345 (2018) 1–9.
[36] O. Rahmanian, M. Dinari, M.K. Abdolmaleki, Carbon quantum dots/layered double hydroxide hybrid for fast and efficient decontamination of Cd(II): The adsorption kinetics and isotherms, Appl. Surf. Sci., 428 (2018) 272–279.
[37] Z. Aksu, Biosorption of reactive dyes by dried activated sludge: equilibrium and kinetic modelling, Biochem. Eng. J., 7 (2001) 79–84.
[38] V. Srivastava, C.H. Weng, V.K. Singh, Y.C. Sharma, Adsorption of nickel ions from aqueous solutions by nano alumina: kinetic, mass transfer, and equilibrium studies, J. Chem. Eng. Data, 56 (2011) 1414–1422.
[39] Y.S. Ho, G. McKay, Pseudo-second order model for sorption processes, Process Biochem., 34 (1999) 451–465.
[40] Y.S. Ho, A.E. Ofomaja, Pseudo-second-order model for lead ion sorption from aqueous solutions onto palm kernel fiber, J. Hazard. Mater., 129 (2006) 137–142.
[41] W.L. Sun, B.F. Jiang, F. Wang, Effect of carbon nanotubes on Cd(II) adsorption by sediments, Chem. Eng. J., 264 (2015) 645–653.
[42] I. Langmuir, The adsorption of gases on plane surfaces of glass, mica, and platinum, J. Am. Chem. Soc., 40 (1918) 1361–1403.
[43] Q.W. Zhou, B.H. Liao, L.N. Lin, W.W. Qiu, Z.G. Song, Adsorption of Cu(II) and Cd(II) from aqueous solutions by ferromanganese binary oxide-biochar composites, Sci. Total Environ., 615 (2018) 115–122.
[44] S. Cataldo, G. Cavallaro, A. Gianguzza, G. Lazzara, A. Pettignano, D. Piazzese, I. Villaescusa, Kinetic and equilibrium study for cadmium and copper removal from aqueous solutions by sorption onto mixed alginate/pectin gel beads, J. Environ. Chem. Eng., 1 (2013) 1252–1260.
[45] H.M.F. Freundlich, Over the adsorption in solution, J. Phys. Chem., 57 (1906) 385–470.
[46] J.C. Echeverria, M.T. Morera, C. Mazkiaran, J.J. Garrido, Competitive sorption of heavy metal by soils. Isotherms and fractional factorial experiments, Environ. Pollut., 101 (1998) 275–284.
[47] D. Gola, P. Dey, A. Bhattacharya, A. Mishra, A. Malik, M. Namburath, S.Z. Ahammad, Multiple heavy metal removal using an entomopathogenic fungi *Beauveria bassiana*, Biores. Technol., 218 (2016) 388–396.
[48] W.A. Jefferson, C.Z. Hu, H.J. Liu, J.H. Qu, Reaction of aqueous Cu-Citrate with MnO_2 birnessite: Characterization of Mn dissolution, oxidation products and surface interactions, Chemosphere, 119 (2015) 1–7.
[49] T.O. Jimoh, A.T. Buoro, M. Muriana, Utilization of *Blighia sapida* (Akee apple) pod in the removal of lead, cadmium and cobalt ions from aqueous solution, J. Environ. Chem. Ecotoxicol., 4 (2012) 178–187.
[50] B. Song, P. Xu, G.M. Zeng, J.L. Gong, X.X. Wang, J. Yan, S.F. Wang, P. Zhang, W.C. Cao, S.J. Ye, Modeling the transport of sodium dodecyl benzene sulfonate in riverine sediment in the presence of multi-walled carbon nanotubes, Water Res., 129 (2018) 20–28.
[51] S.J. Lee, J.H. Park, Y.T. Ahn, J.W. Chung, Comparison of heavy metal adsorption by peat moss and peat moss-derived biochar produced under different carbonization conditions, Water Air Soil Pollut., 226 (2015) 9–19.
[52] Y.A. Zheng, S.B. Hua, A.Q. Wang, Adsorption behavior of Cu^{2+} from aqueous solutions onto starch-g-poly (acrylic acid)/sodium humate hydrogels, Desalination, 263 (2010) 170–175.

[53] B. Song, G.M. Zeng, J.L. Gong, P. Zhang, J.Q. Deng, C.H. Deng, J. Yan, P. Xu, C. Lai, C. Zhang, M. Cheng, Effect of multi-walled carbon nanotubes on phytotoxicity of sediments contaminated by phenanthrene and cadmium, Chemosphere, 172 (2017) 449–458.
[54] A.T. Paulino, L.A. Belfiore, L.T. Kubota, E.C. Muniz, E.B. Tambourgi, Efficiency of hydrogels based on natural polysaccharides in the removal of Cd^{2+} ions from aqueous solutions, Chem. Eng. J., 168 (2011) 68–76.
[55] K.V. Kumar, Optimum sorption isotherm by linear and non-linear methods for malachite green onto lemon peel, Dyes Pigments, 74 (2007) 595–597.
[56] A. Kaushik, H.R. Sharma, S. Jain, J. Dawra, C.P. Kaushik, Pesticide pollution of River Ghaggar in Haryana, India, Environ. Monit. Assess., 160 (2010) 61–69.